

Traveling Slow Waves of Neural Activity: A Novel Form of Network Activity in Developing Neocortex

Alejandro Peinado

Department of Neuroscience, Albert Einstein College of Medicine, Bronx, New York 10461

Spontaneous neuronal firing during development has the potential to shape many aspects of neuronal wiring throughout the brain. Bursts of electrical activity coordinated among large numbers of neurons, occurring during a brief developmental window, have been described in many regions of the CNS, including retina, hippocampus, and spinal cord, but evidence for this type of activity in developing neocortex has so far been lacking. To identify conditions that may give rise to patterned spontaneous electrical activity in developing neocortex, cholinergic agonists were applied to immature rat cortical slices while large-scale activity was imaged optically with fura-2 AM. Here I show that activation of muscarinic acetylcholine receptors results in waves of correlated neural activity. Waves recruit large numbers of neurons, are slowly propagating, regenerative events involving depolarization and associated calcium trans-

sients, and advance for many millimeters as a sharp wave front perpendicular to the pial surface, at speeds ranging between 50 and 300 $\mu\text{m}/\text{sec}$. The expression of waves is restricted temporally to a brief period in postnatal development, until postnatal day 6, and spatially to some neocortical areas. The ability of isolated neocortical networks to generate large-scale patterned activity endogenously during a period of massive neurite extension and synaptogenesis raises the possibility that at least in some cortical areas these processes might be influenced by patterned neuronal firing generated independently of thalamocortical input.

Key words: spontaneous activity; waves; neocortex; acetylcholine; muscarinic; calcium; fura-2; voltage-sensitive dyes; patch clamp; imaging

The complex neural circuits of the cerebral cortex and the connections between them and other parts of the nervous system are constructed over an extended period, both before and after birth, during which genetically programmed molecular cues and electrical activity interact in as yet poorly understood ways to guide axons to their targets and refine patterns of synaptic connectivity. The role of activity in circuit formation was first shown in the visual system with the demonstration that controlled changes in visual experience modify the pattern of projections from thalamus to cortex in stereotyped ways (Wiesel, 1982). Subsequent to this finding, other investigations have revealed that activity-dependent developmental processes are operating and might contribute to circuit formation in sensory pathways even before the time when sensory stimulation becomes a major driving force behind the activation of those pathways (Rakic, 1976; Stryker and Harris, 1986; Sretavan et al., 1988). This apparent paradox has led more recently to an interest in the presence of endogenous activation in immature circuits and the spatiotemporal patterns characteristic of this type of activity. Characterization of the various modes of endogenous circuit activation now seems essential for understanding the full extent of the role that activity plays in shaping aspects of circuit development as diverse as gene expression (Buonanno and Fields, 1999), axonal pathfinding (Catalano and Shatz, 1998; Dantzker and Callaway, 1998), and circuit refinement (Ruthazer and Stryker, 1996; Penn et al., 1998; Cook et al., 1999). The results of this study demonstrate that, at

least *in vitro*, endogenous patterned electrical activity can arise in immature neocortical circuits in response to cholinergic activation.

MATERIALS AND METHODS

Long-Evans rat pups aged 0–10 d (day 0 = day of birth) were used to prepare 300- μm -thick brain slices. The plane of section was coronal, and slices were made to include the parietal region. No attempt was made to distinguish among functional areas within parietal cortex. Slices were incubated in artificial CSF (aCSF) containing fura-2 AM (5 $\mu\text{g}/\text{ml}$) for 1–2 hr at 30°C. Composition of the aCSF was (in mM): NaCl 125, KCl 2.5, NaHCO₃ 26, KH₂PO₄ 1.25, MgCl₂·6H₂O 1, CaCl₂ 2, D-glucose, 10, pH 7.4, bubbled with O₂/CO₂. Slices were then placed on a temperature-controlled (30 \pm 1°C) perfusion chamber (rate: 2–3 ml/min.; volume: 200–400 μl) on the microscope (Zeiss Axioskop FS) stage and viewed with a 20 \times water-immersion objective. A 0.5 \times magnification adapter was placed in front of the camera to obtain a larger (750 \times 750 μm) image area. Optical recordings were made using a cooled CCD digital camera (512 EFT, Princeton Instruments) and IPLab Software (Scanalytics). For single-wavelength acquisition, image sequences consisted of 700 frames and were acquired continuously for 140 sec (200 msec integration time per frame). Camera was operated on 4 \times 4 pixel binning mode. All fluorescence measurements were taken from regions of interest contain-

Received Sept. 17, 1999; revised Nov. 2, 1999; accepted Nov. 10, 1999.

This work was supported by grants from National Institutes of Health (MH53345 and NS319899). I thank Drs. Scott Nawy and Don Faber for helpful discussions.

Correspondence should be addressed to Alejandro Peinado, Department of Neuroscience, Room 522, Kennedy Center, Albert Einstein College of Medicine, 1300 Morris Park Avenue, Bronx, NY 10461. E-mail: peinado@aecom.yu.edu.

Copyright © 1999 Society for Neuroscience 0270-6474/99/200001-06\$15.00/0

This article is published in *The Journal of Neuroscience*, Rapid Communications Section, which publishes brief, peer-reviewed papers online, not in print. Rapid Communications are posted online approximately one month earlier than they would appear if printed. They are listed in the Table of Contents of the next open issue of *JNeurosci*. Cite this article as: *JNeurosci*, 2000, 20:RC54 (1–6). The publication date is the date of posting online at www.jneurosci.org.

<http://www.jneurosci.org/cgi/content/full/3858>

ing multiple neurons and represent average pixel intensity over time for regions $\sim 50 \times 50 \mu\text{m}$ located in supragranular layers.

All fura-2 wave activity was recorded at a single excitation wavelength using a $380 \pm 5 \text{ nm}$ bandpass filter. Control experiments recorded using a $360 \pm 5 \text{ nm}$ excitation filter (isosbestic point for fura-2) showed no signals in response to cholinergic agonists. Emission fluorescence was filtered with a 400 nm longpass filter.

For imaging of voltage signals, slices were stained for 5 min with the voltage-sensitive dye di-4-ANEPPS (Fluhler et al., 1985) (0.66 mg/ml in aCSF) while in the perfusion chamber, and only after a wave-expressing region had been located using fura-2 imaging. Wave activity was imaged immediately, after a 5 min wash period, to minimize artifactual signals attributable to gradual internalization of the dye and photodynamic damage (Schaffer et al., 1994). For dual fura-2/di-4-ANEPPS recordings excitation filters (380 ± 5 and $546 \pm 5 \text{ nm}$) were alternated every 0.5 sec, and a single emission filter (590 nm longpass) was used. Neutral density filters were used to equalize fura-2 and di-4-ANEPPS signal intensities and to minimize photobleaching.

For whole-cell current-clamp recordings, patch pipettes were pulled from borosilicate glass ($3\text{--}5 \text{ M}[\text{SCAP}]\Omega$) and filled with an internal solution containing (in mM): K gluconate 110, KCl 20, HEPES 10, EGTA 10, CaCl_2 1, MgCl_2 1, pH 7.2; osmolarity was adjusted to 307 mOsm with sucrose. Signals were amplified with an Axopatch 200A patch-clamp amplifier (Axon Instruments) and acquired using Synapse (Synergy Research) and an ITC-16 computer interface (Instrutech Corporation).

Drug application was synchronized to imaging using Synapse and began 10 sec after the start of imaging to allow acquisition of baseline fluorescence values. The interval between applications was at least 5 min.

RESULTS

Fluorescence imaging at low magnification was used to visualize population activity in coronal slices of immature rat neocortex stained with the cell-permeant calcium indicator dye fura-2 AM. Under control conditions, no large-scale patterned activity was observed in immature neocortical slices. The rationale for testing cholinergic agonists in neocortex was that in retina, blockade of nicotinic acetylcholine receptors eliminates spontaneous activity waves, suggesting that acetylcholine is necessary for their expression (Feller et al., 1996). To mimic activation of cholinergic inputs to neocortex in slices, where such inputs are not preserved, the nicotinic and muscarinic cholinergic agonist carbachol (CCh) was bath-applied for periods varying in length from 5 to 60 sec while activity was being recorded optically over a $750 \times 750 \mu\text{m}$ area of neocortex.

The results obtained with CCh are described below along with results obtained with the cholinergic agonist muscarine, which was used to determine whether the cholinergic involvement was mediated through muscarinic or nicotinic receptors. Although both nicotinic and muscarinic receptors are present and functional in immature neocortex (van Huizen et al., 1994; Roerig et al., 1997), experiments using muscarine yielded results that are indistinguishable from results obtained with CCh.

Application of CCh ($25 \mu\text{M}$) or muscarine ($20 \mu\text{M}$) to 60 coronal slices that included parietal cortex resulted in waves being recorded at 93 of 302 cortical sites (31%). Typically, activity waves originated somewhere outside the camera's field of view, entered at one edge of the imaged area, and continued their advance outside this area (Fig. 1A). The direction of wave advance was always parallel to the pial surface. The wave front, which is therefore oriented perpendicular to the cortical layering, moves at speeds that range between 50 and $300 \mu\text{m}/\text{sec}$ ($125 \pm 64 \mu\text{m}/\text{sec}$, mean \pm SD, $n = 60$ waves). In several instances the imaged area happened to include the site of wave initiation, enabling the initial evolution of a wave to be captured in 200-msec-long snapshots (Fig. 1B). These sequences show that although agonist is applied throughout the slice, a wave starts from an event involving a very small number of cells from where

activity radiates outward until a full-fledged horizontally moving wavefront is attained, sometimes traveling for distances in excess of 3 mm.

Graphic presentation of the time course of calcium-dependent fura-2 fluorescence changes (Fig. 1C) shows that the response to cholinergic agonist has two phases. First, a few seconds after switching from normal superfusion solution to agonist-containing solution, a small increase ($4\text{--}10\%$ $\Delta F/F$) in intracellular calcium occurs in large numbers of cells throughout the extent of the imaged area. This phase of the response occurs simultaneously throughout the field of view, peaks within 5–10 sec, and decays slowly to baseline over the next minutes even in the continuous presence of agonist, as has been shown previously (Yuste and Katz, 1991). The second phase of the response, when it shows up, appears with a highly variable delay and is significantly larger ($10\text{--}20\%$ $\Delta F/F$), possibly because more neurons are involved per sampled area. When the time course of signals derived from two sites positioned along the horizontal extent of cortex are aligned, the second phase, but not the first, consistently shows a lag in onset at one site relative to the other (Fig. 1C). This calcium transient, corresponding to the traveling wave, has a fast rise and almost equally fast decay and invariably rides on the short-latency, lower-amplitude phase of the cholinergic response.

As expected, the broad spectrum muscarinic antagonist atropine ($1 \mu\text{M}$) blocked the response to muscarine and CCh ($n = 5$ slices). To further narrow the receptor subtype involved in the muscarinic response, four subtype-selective receptor antagonists were tested. Antagonists to m1 (pirenzepine, 100 nM ; $n = 4$) and m3 (4-DAMP, 2.5 nM ; $n = 5$) both blocked muscarine-induced waves in every instance (Fig. 1D). Antagonists to m2 (gallamine, $20 \mu\text{M}$; $n = 3$) and m4 (MT-3, 10 nM ; $n = 2$) failed to block muscarine-induced waves. In the case of MT-3, however, it is unclear whether, despite a 30 min preincubation, the large toxin (molecular weight 7289.3 Da) gained sufficient access into the slice.

To investigate the relationship between age and incidence of wave expression in developing neocortex, CCh or muscarine was applied to slices from rats aged 0–9 d postnatal (P0–9). Data for each age group were analyzed in terms of fraction of cortical sites where at least one wave was elicited on superfusion of agonist (Fig. 2A). Typically (92% of cases), sites were of one of two types: those in which waves were elicited repeatedly on repeated agonist application, and those in which waves could not be elicited despite repeated applications of agonist. Both types of sites were found to coexist in individual slices until P6–7. After P7, agonist application induced a short-latency, small-amplitude response but no waves.

The finding that wave-expressing and nonexpressing sites can coexist in single slices suggests that there are mechanisms within cortex that restrict the propagation of waves to specific areas. This idea is supported by 35 recordings in which waves were observed to end within the field of view (Fig. 2B). Although no obvious cytoarchitectonic discontinuities could be observed at these sites, it is not possible to determine in fura-2-stained slices whether wave termination correlates with some functional boundary in cortex. An interesting feature of wave termination sites in cortex is that they can be stable for periods in excess of 1 hr (Fig. 2B).

To find out whether cholinergically induced waves involve electrical activity, three types of experiments were performed. First, muscarine responses were evoked in slices stained with both fura-2 AM and the voltage-sensitive dye di-4-ANEPPS. Dual calcium and voltage recordings in these slices ($n = 5$) demonstrate

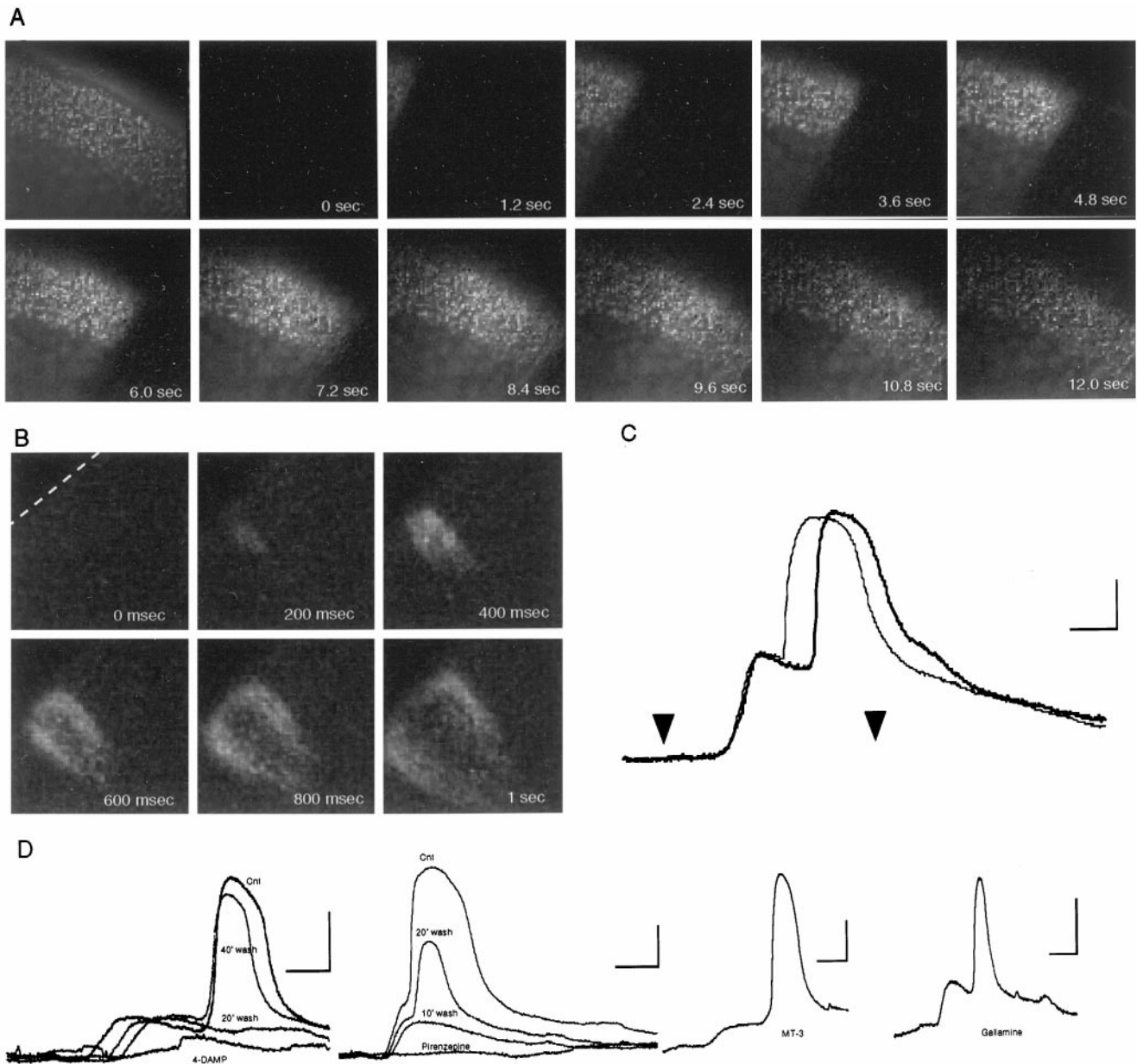


Figure 1. Cholinergic agonists evoke waves of correlated calcium transients in developing rat neocortical slices through activation of muscarinic receptors. *A*, Time-lapse sequence of changes in calcium-dependent fura-2 fluorescence during carbachol ($25 \mu\text{M}$) superfusion in a P5 slice. Pial edge is the *top right margin*. First frame (*top left*) shows fura-2 fluorescence staining of imaged cortical region in coronal section (cut across cortical layers). Subsequent frames are difference images showing a wave advancing over this area of cortex. *White areas* represent cells with largest fluorescence change relative to prewave levels. Image dimensions (*A, B*) are $750 \times 750 \mu\text{m}$. *B*, Initiation of wave at a different cortical site shown at 200 msec intervals. *Dashed line* on first frame marks the pial edge of the slice. *White areas* represent cells with fluorescence changes relative to previous frame. *C*, Plot of changes in calcium-dependent fura-2 fluorescence over time recorded at two sites situated $400 \mu\text{m}$ apart along the path of wave advance. *Arrowheads* show beginning and end of $20 \mu\text{M}$ muscarine chloride application for 60 sec. Calibration in *C*: $5\% \Delta F/F$, 10 sec. *D*, Antagonists for the m1 (pirenzepine, $0.1 \mu\text{M}$) and m3 (4-DAMP, 2.5 nM) receptor subtypes, but not the m2 (gallamine, $20 \mu\text{M}$) or m4 (MT-3, 10 nM) subtypes, reversibly abolished muscarine-evoked activity waves. Calibration in *D*: $5\% \Delta F/F$, 20 sec.

that a voltage signal can be detected that is simultaneous with the high amplitude, wave-associated calcium signal (Fig. 3*A*), indicative of depolarization during waves. In contrast, no measurable voltage signal is detected in association with the initial, low-amplitude part of the cholinergic response. Second, current-clamp recordings from individual neurons also show that during the passage of a wave, neurons fire a burst of action potentials (Fig. 3*B*). Finally, a requirement for depolarization and action potential firing during waves was demonstrated by experiments in

which waves were induced before and during superfusion with the sodium channel blocker tetrodotoxin (TTX) ($n = 7$). TTX eliminates the wave-associated calcium transient and leaves the initial, smaller calcium response relatively unaffected (Fig. 3*C*). The presence of electrical activity during waves suggests that the potential influence of activity waves on the development of neocortex could go beyond an effect on the local circuitry to include longer-range projections as well. The TTX sensitivity of cholinergically induced waves also demonstrates that this phenomenon

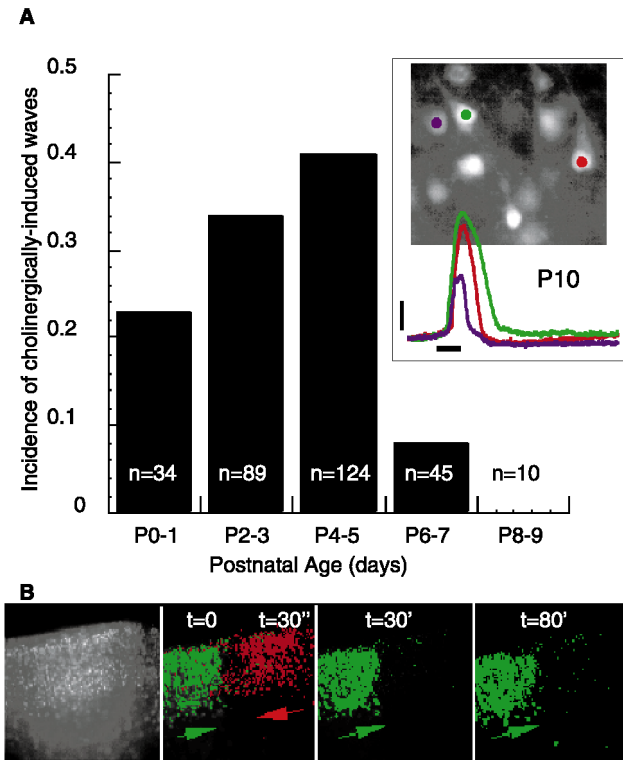


Figure 2. Expression of cholinergically induced waves is restricted developmentally and spatially. *A*, Histogram showing the fraction of sites at which one or more waves could be elicited with cholinergic agonists at each age group. Data include waves elicited with $25 \mu\text{M}$ CCh ($n = 208$) or $20 \mu\text{M}$ muscarine ($n = 94$). *Inset*, Fura-2 signals from three representative neurons (identified by their prominent apical dendrite) in response to a 15 sec application of $50 \mu\text{M}$ glutamate (*horizontal bar*) to a P10 slice demonstrate that the age-related decrease in waves is not caused by a technical problem with fura-2 signaling. Vertical bar, $5\% \Delta F/F$. *B*, An example of a wave propagation boundary in developing neocortex. *Leftmost frame* shows raw fura-2 fluorescence image of cortical area shown in subsequent frames. Note absence of any obvious cytoarchitectonic boundary. Successive waves induced in this cortical area (extent of area traversed shown in *green* or *red*) show that boundaries can exist between subregions of cortex even when both subregions express wave activity, and that boundaries can be stable over time. Time of occurrence is shown above each wave. *Arrows* under each wave show direction of advance. Image dimensions are $750 \times 750 \mu\text{m}$.

is pharmacologically distinct from domains in developing neocortex (Yuste et al., 1992) and from spreading depression (Sugaya et al., 1975; Tobiasz and Nicholson, 1982).

Acetylcholine acting through muscarinic receptors has been shown to depolarize mature cortical neurons (McCormick, 1993). To test whether large-scale depolarization of neurons in developing neocortex is a sufficient stimulus for induction of waves, an excitatory neurotransmitter, glutamate, was superfused instead of one of the two cholinergic agonists during calcium imaging at sites previously determined to express waves with muscarine ($n = 5$). The glutamate stimulus, although capable of inducing a significant calcium response, was unable to induce waves at these sites (Fig. 4*A*).

To test the involvement of glutamatergic neurotransmission in the spread of activity during waves, two ionotropic glutamate receptor antagonists, APV (NMDA; $25 \mu\text{M}$) and CNQX (non-NMDA; $25 \mu\text{M}$), were bath-applied simultaneously during, as well as for 10 min before, the application of muscarine ($n = 6$). As shown in Figure 4*B*, neurotransmission via ionotropic glutamate receptors is not required for wave induction or propagation.

DISCUSSION

In the present study I have described the most salient features of a newly discovered type of network activity in immature neocortex, including its developmental profile, its spatiotemporal characteristics, and the muscarinic receptor subtypes involved in its induction. Bursting patterns of neural activity similar to that described here have been demonstrated in other immature neural circuits including retina (Maffei and Galli-Resta, 1990; Meister et al., 1991), spinal cord (O'Donovan et al., 1994; Milner and Landmesser, 1999), and hippocampus (Ben-Ari et al., 1989; Garaschuk et al., 1998; Avignone and Cherubini, 1999) (for review, see O'Donovan, 1999). Acetylcholine is often involved in this activity, sometimes via nicotinic (retina, spinal cord) and sometimes via muscarinic (hippocampus, neocortex) receptors. As in other brain regions, cholinergic sources in neocortex are present early (Dori and Parnavelas, 1989).

Much remains to be elucidated about the mechanisms responsible for activity waves in neocortex. The type(s) of intercellular signaling involved in wave propagation, for example, remains to be established. The finding that ionotropic glutamate receptors do not appear to be necessary is not too surprising in light of knowledge about other excitatory mechanisms potentially available to immature neocortical networks, including signaling via glycine, GABA_A and metabotropic glutamate receptors, and gap

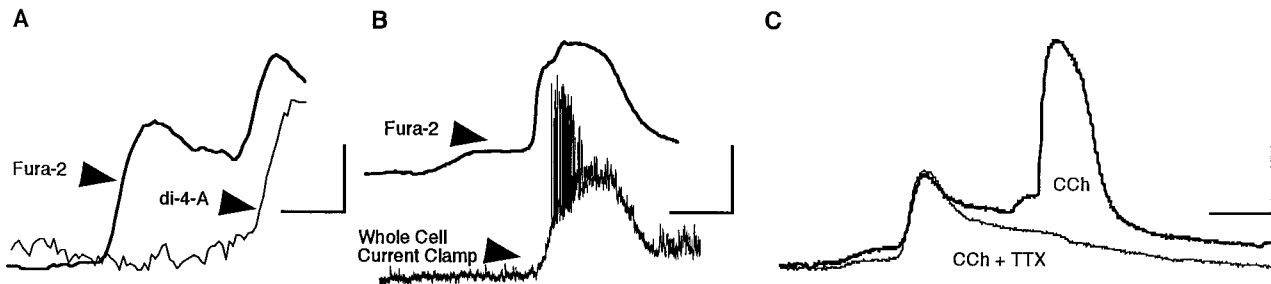


Figure 3. Cholinergic waves are excitatory events involving neuronal depolarization and firing. *A*, Simultaneous calcium and voltage imaging during cholinergic stimulation. A change in fluorescence signal, consistent with depolarization, occurs in the voltage-sensitive dye di-4-ANEPPS (*di-4-A*) concurrent with the wave-related calcium transient (*second peak* in fura-2 trace). *B*, Whole-cell current-clamp recording from a layer 2/3 neuron (*bottom trace*) obtained during a muscarine-evoked wave, as shown in the simultaneous fura-2 response (*top trace*). *C*, Blockade of the wave-related fura-2 fluorescence transient, but not of the slower cholinergic response, by the sodium channel blocker tetrodotoxin (*TTX*, $1 \mu\text{M}$). Calibration: $10\% \Delta F/F$, 10 sec (*A*); $10\% \Delta F/F$, 25 mV , 10 sec (*B*); $10\% \Delta F/F$, 20 sec (*C*).

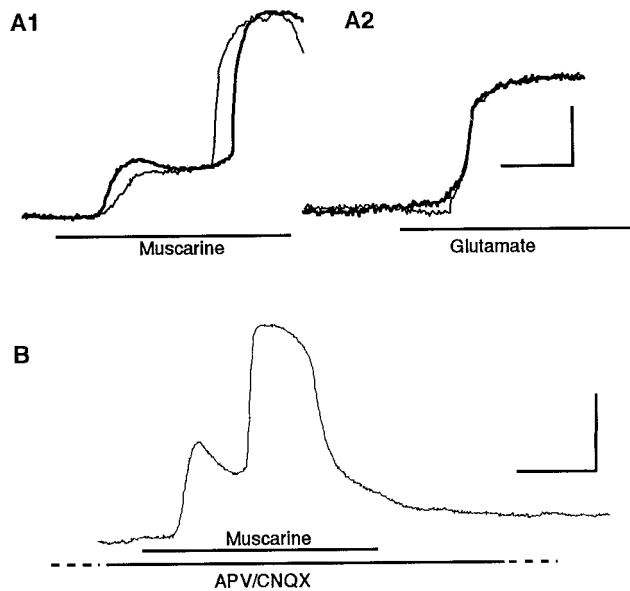


Figure 4. Ionotropic glutamate receptor activation is neither necessary nor sufficient for induction of neocortical waves. *A*, Comparison of responses to muscarine (20 μ M) and glutamate (20 μ M) at a single cortical site. The two traces in each panel are mean fluorescence values over time from two small regions of interest separated by 400 μ m. Unlike muscarine (*A1*), which induces a traveling calcium transient, glutamate (*A2*) induces a calcium transient that occurs simultaneously throughout the slice (as shown by superposition of traces from the two regions of interest). *B*, Muscarine-induced wave in the presence of APV (25 μ M) and CNQX (25 μ M). Calibration: 20 msec, 5% $\Delta F/F$.

junctions (Peinado et al., 1993; Owens et al., 1996; Flint et al., 1998). Unlike glutamate, these mechanisms are expressed transiently in neocortex. Their involvement therefore could also account for the developmental profile of wave activity seen here. To determine what mechanisms are involved in wave propagation, however, an experimental approach is needed that can separate effects on wave propagation from effects on wave initiation, an objective that cannot be accomplished through application of receptor antagonists to the entire slice as was done here.

The inability of bath-applied glutamate to induce wave activity suggests that for waves to occur the neural network may need to undergo a transient change in excitability state in addition to depolarization. One possibility is a switch into a burst-ready mode, in which neurons are more likely to burst-fire in response to excitatory input; another could be an enhancement in neurotransmitter release. Activation of muscarinic receptors could accomplish either of these by reducing specific potassium conductances (McCormick, 1993). Even if such an effect by muscarinic receptors can be demonstrated during wave activity, however, a complete description of wave physiology is unlikely to emerge until the wave initiation foci can be characterized more fully in terms of physiological properties unique to these sites.

The results presented here raise the intriguing possibility that activity waves in immature neocortex may function *in vivo*, albeit in as yet unknown ways, as participants in the formation of cortical circuits. An alternative interpretation of these results, one that has been favored in interpreting different types of large-scale neuronal bursting behavior induced by GABA_A antagonists, potassium channel blockers, or low [Mg²⁺]_o, is that this is an example of epileptic activity that is unlikely to occur *in vivo* except as pathology. The possibility that muscarine-induced waves are

also unphysiological cannot be ruled out at this stage. The evidence from retina and spinal cord, however, suggests not only that limited seizure-like neuronal bursting at specific stages of cortical development may not be deleterious, but that it might in fact be useful.

REFERENCES

- Avignone E, Cherubini E (1999) Muscarinic receptor modulation of GABA-mediated giant depolarizing potentials in the neonatal rat hippocampus. *J Physiol (Lond)* 518:97–107.
- Ben-Ari Y, Cherubini E, Corradetti R, Gaiarsa JL (1989) Giant synaptic potentials in immature rat CA3 hippocampal neurones. *J Physiol (Lond)* 416:303–325.
- Buonanno A, Fields RD (1999) Gene regulation by patterned electrical activity during neural and skeletal muscle development. *Curr Opin Neurobiol* 9:110–120.
- Catalano SM, Shatz CJ (1998) Activity-dependent cortical target selection by thalamic axons. *Science* 281:559–562.
- Cook PM, Prusky G, Ramoa AS (1999) The role of spontaneous retinal activity before eye opening in the maturation of form and function in the retinogeniculate pathway of the ferret. *Vis Neurosci* 16:491–501.
- Dantzker JL, Callaway EM (1998) The development of local, layer-specific visual cortical axons in the absence of extrinsic influences and intrinsic activity. *J Neurosci* 18:4145–4154.
- Dori I, Parnavelas JG (1989) The cholinergic innervation of the rat cerebral cortex shows two distinct phases in development. *Exp Brain Res* 76:417–423.
- Feller MB, Wellis DP, Stellwagen D, Werblin FS, Shatz CJ (1996) Requirement for cholinergic synaptic transmission in the propagation of spontaneous retinal waves. *Science* 272:1182–1187.
- Flint AC, Liu X, Kriegstein AR (1998) Nonsynaptic glycine receptor activation during early neocortical development. *Neuron* 20:43–53.
- Fluhler E, Burnham VG, Loew LM (1985) Spectra, membrane binding, and potentiometric responses of new charge shift probes. *Biochemistry* 24:5749–5755.
- Garaschuk O, Hanse E, Konnerth A (1998) Developmental profile and synaptic origin of early network oscillations in the CA1 region of rat neonatal hippocampus. *J Physiol (Lond)* 507:219–236.
- Maffei L, Galli-Resta L (1990) Correlation in the discharges of neighboring rat retinal ganglion cells during prenatal life. *Proc Natl Acad Sci USA* 87:2861–2864.
- McCormick DA (1993) Actions of acetylcholine in the cerebral cortex and thalamus and implications for function. *Prog Brain Res* 98:303–308.
- Meister M, Wong RO, Baylor DA, Shatz CJ (1991) Synchronous bursts of action potentials in ganglion cells of the developing mammalian retina. *Science* 252:939–943.
- Milner LD, Landmesser LT (1999) Cholinergic and GABAergic inputs drive patterned spontaneous motoneuron activity before target contact. *J Neurosci* 19:3007–3022.
- O'Donovan M, Ho S, Yee W (1994) Calcium imaging of rhythmic network activity in the developing spinal cord of the chick embryo. *J Neurosci* 14:6354–6369.
- O'Donovan MJ (1999) The origin of spontaneous activity in developing networks of the vertebrate nervous system. *Curr Opin Neurobiol* 9:94–104.
- Owens DF, Boyce LH, Davis MB, Kriegstein AR (1996) Excitatory GABA responses in embryonic and neonatal cortical slices demonstrated by gramicidin perforated-patch recordings and calcium imaging. *J Neurosci* 16:6414–6423.
- Peinado A, Yuste R, Katz LC (1993) Extensive dye coupling between rat neocortical neurons during the period of circuit formation. *Neuron* 10:103–114.
- Penn AA, Riquelme PA, Feller MB, Shatz CJ (1998) Competition in retinogeniculate patterning driven by spontaneous activity. *Science* 279:2108–2112.
- Rakic P (1976) Prenatal genesis of connections subserving ocular dominance in the rhesus monkey. *Nature* 261:467–471.
- Roerig B, Nelson DA, Katz LC (1997) Fast synaptic signaling by nicotinic acetylcholine and serotonin 5-HT₃ receptors in developing visual cortex. *J Neurosci* 17:8353–8362.
- Ruthazer ES, Stryker MP (1996) The role of activity in the development

- of long-range horizontal connections in area 17 of the ferret. *J Neurosci* 16:7253–7269.
- Schaffer P, Ahammer H, Muller W, Koidl B, Windisch H (1994) Di-4-ANEPPS causes photodynamic damage to isolated cardiomyocytes. *Pflügers Arch* 426:548–551.
- Sretavan DW, Shatz CJ, Stryker MP (1988) Modification of retinal ganglion cell axon morphology by prenatal infusion of tetrodotoxin. *Nature* 336:468–471.
- Stryker MP, Harris WA (1986) Binocular impulse blockade prevents the formation of ocular dominance columns in cat visual cortex. *J Neurosci* 6:2117–2133.
- Sugaya E, Takato M, Noda Y (1975) Neuronal and glial activity during spreading depression in cerebral cortex of cat. *J Neurophysiol* 38:822–841.
- Tobiasz C, Nicholson C (1982) Tetrodotoxin resistant propagation and extracellular sodium changes during spreading depression in rat cerebellum. *Brain Res* 241:329–333.
- van Huizen F, March D, Cynader MS, Shaw C (1994) Muscarinic receptor characteristics and regulation in rat cerebral cortex: changes during development, aging and the oestrous cycle. *Eur J Neurosci* 6:237–243.
- Wiesel TN (1982) Postnatal development of the visual cortex and the influence of environment. *Nature* 299:583–591.
- Yuste R, Katz LC (1991) Control of postsynaptic Ca^{2+} influx in developing neocortex by excitatory and inhibitory neurotransmitters. *Neuron* 6:333–344.
- Yuste R, Peinado A, Katz LC (1992) Neuronal domains in developing neocortex. *Science* 257:665–669.